

## BUILDING SHAPE FUNCTIONS ON CONVEX POLYHEDRA USING MLS INTERPOLANTS AND RATIONAL WEIGHTS

Gloria Simonetti and Carlos Zuppa\*

\*Departamento de Matemáticas. UNSL.  
Chacabuco y Pedernera. 5700. San Luis. Argentina.  
e-mail: zuppa@unsl.edu.ar, web page: <http://liaem0.unsl.edu.ar/lmc/>

**Abstract.** *A method for building  $C^0$  shape functions on convex polyhedra using moving least square interpolation with rational weights is introduced. These natural interpolants are presented and their use in a meshless FEM scheme for the solutions of elliptic PDEs is discussed. Numerical experiments are provided to demonstrate the utility and robustness of the proposed method.*

**Key Words:** meshless methods, moving least square interpolation, rational weights.

## 1 INTRODUCTION

Recent developments in the context of meshless finite element methods have demonstrated the importance of the implementation of trial and test functions over polyhedral regions<sup>1,2,3</sup>. In these methods, polyhedral divisions of the domain given by means of a set of fixed nodes are made, fundamentally with the help of Voronoy tessellations, or Delaunay triangulations. Some cosmetic is then applied in the mesh in order to eliminate slivers. In the natural element method, Sibson coordinates are used to construct shape functions and meshless interpolants.

In this paper, we discuss the construction of continuous shape functions over convex polyhedra using moving least square interpolants with rational weights (nemlsq). This methodology produces accurate results in Galerkin schemes for solving PDEs in hybrid meshes, as overlapping grids systems<sup>4</sup>.

The method can also be used to build discontinuous (Haar) and other catastrophic shape functions, but we shall not deal with this problem in the present paper<sup>5</sup>.

Several numerical results are presented that show that this methodology can be an appealing choice to construct element interpolants in meshless finite element methods and hybrid grids.

## 2 THE METHOD

We consider bounded convex polyhedron  $E \subset \mathbb{R}^n$  defined by

$$E = \{\mathbf{x} \in \mathbb{R}^n : f_\alpha(x) \geq 0, \alpha = 1, \dots, N\} \tag{1}$$

where  $f_\alpha(\mathbf{x}) = A_\alpha \cdot \mathbf{x} + B_\alpha$  (the dot means the standard scalar product in  $\mathbb{R}^n$ ). The boundary  $\partial E$  can be decomposed into the union of the  $r$ -facets of  $E$ ,  $r = 0, \dots, n-1$ . The  $0$ -facets are the nodes  $\{\mathbf{z}_\gamma\}_{\gamma=1}^M$  of  $E$ . We assume that the closure of every  $(n-1)$ -facet is obtained as the intersection  $\{f_\alpha(\mathbf{x}) = 0\} \cap E$ , for some  $\alpha \in \{1, \dots, N\}$  and the convex hull

$$[\mathbf{z}_1, \dots, \mathbf{z}_M] = E$$

is not generated for any proper subset of  $\{\mathbf{z}_1, \dots, \mathbf{z}_M\}$ . That is, we shall admit elements as those shown in figure 1.a, but not as in figure 1.b. A work in progress deals with case (b).

For every  $\gamma = 1, \dots, M$ , let  $\{\beta_1, \dots, \beta_\gamma\}$  be the subset of  $\{1, \dots, N\}$  such that the  $(n-1)$ -facets  $\{f_{\beta_j}(\mathbf{x}) = 0\} \cap E$ ,  $j = 1, \dots, \gamma$  share node  $\mathbf{z}_\gamma$ ,  $\phi_\gamma$  the rational function defined by

$$\phi_\gamma(\mathbf{x}) = \frac{1}{f_{\beta_1}(\mathbf{x}) \cdot \dots \cdot f_{\beta_\gamma}(\mathbf{x})} \tag{2}$$

and

$$\omega_\gamma(\mathbf{x}) = \frac{\phi_\gamma(\mathbf{x})}{\sum_{\nu=1}^M \phi_\nu(\mathbf{x})}$$

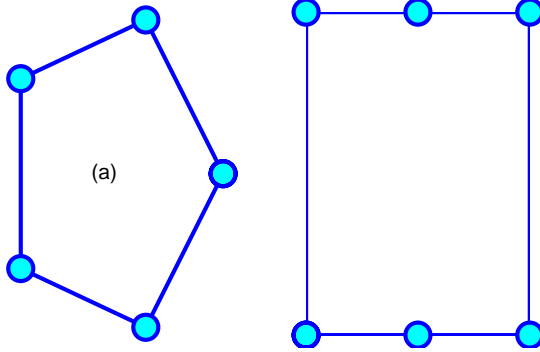


Figure 1: Admissible element (a) and non admissible (b)

Functions  $\{\omega_\gamma\}$  are, at least, defined in the interior  $E^\circ$  of  $E$ .

It can be proved that the values  $\omega_\gamma(\mathbf{y}_m)$ ,  $\gamma$  fixed, tend to a definite value when  $\mathbf{y}_m \rightarrow \mathbf{y} \in \partial E$ . In particular, for every  $\gamma = 1, \dots, M$ ,  $\omega_\gamma(y_m) \rightarrow \delta_{\gamma\zeta}$  if  $\mathbf{y}_m \rightarrow \mathbf{z}_\zeta$ .

Let  $\mathbf{f} = \{f_\gamma\}$  be some set of real values on *nodes*  $\{\mathbf{z}_\gamma\}$ ,  $\mathbf{x}$  an interior point in  $E$ ,  $P_{(\mathbf{f},\mathbf{x})}$  the linear polynomial

$$a_0 + \mathbf{a}_1 \cdot (\mathbf{X} - \mathbf{x}) \tag{3}$$

which minimizes the functional

$$J_{(f,\mathbf{x})}(a_0, \mathbf{a}_1) = \frac{1}{2} \sum_{\gamma=1}^M \omega_\gamma(\mathbf{x}) (a_0 + \mathbf{a}_1 \cdot (\mathbf{z}_\gamma - \mathbf{x}) - f_\gamma)^2 \tag{4}$$

and  $\psi_{\mathbf{f}}$  the function defined by formula

$$\psi_{\mathbf{f}}(\mathbf{x}) = P_{(\mathbf{f},\mathbf{x})}(\mathbf{x}) = a_0(\mathbf{x}) \tag{5}$$

The operator  $\mathbf{f} \rightarrow \psi_{\mathbf{f}}$  is linear. Then, if  $\{\mathbf{e}_\gamma\}_{\gamma=1,\dots,M}$  is the standard basis of  $\mathbb{R}^M$ , we have

$$\psi_{\mathbf{f}} = \sum_{\gamma=1}^M f_\gamma \psi_\gamma$$

where we have denoted  $\psi_\gamma = \psi_{\mathbf{e}_\gamma}$ .

If  $B, W$  are the matrices

$$B = \begin{pmatrix} 1 & \mathbf{z}_1 - \mathbf{x} \\ \vdots & \vdots \\ 1 & \mathbf{z}_M - \mathbf{x} \end{pmatrix}$$

$$W = \begin{pmatrix} \omega_1(\mathbf{x}) & 0 & \cdots & 0 \\ 0 & \omega_2(\mathbf{x}) & \cdots & 0 \\ \vdots & \vdots & \ddots & 0 \\ 0 & \cdots & 0 & \omega_\gamma(\mathbf{x}) \end{pmatrix}$$

it is well known<sup>9</sup> that coefficients  $\hat{\mathbf{a}} = (a_0, \mathbf{a}_1)$  in (4) are obtained from

$$\hat{\mathbf{a}} = (BWB^T)^{-1} B^T W \mathbf{f} \tag{6}$$

and the partial derivatives  $D_k \hat{\mathbf{a}}, k = 1, \dots, n$ , are

$$D_k \hat{\mathbf{a}} = (BWB^T)^{-1} B^T (D_k W)(\mathbf{f} - B \cdot \hat{\mathbf{a}})$$

From (5) one can easily see that

$$D_k \psi_{\mathbf{f}} = D_k a_0 + (\mathbf{a}_1)_k, \quad k = 1, \dots, n$$

Functions  $\{\psi_\gamma\}_{\gamma=1, \dots, M}$  are the shape functions of element  $E$ . A number of things must be proved before we accept that the behavior of functions  $\{\psi_\gamma\}$  are those one hopes for shape functions. We list the principal properties of  $\{\psi_\gamma\}$  :

- If  $\{\mathbf{x}_m\} \subset E^\circ$  and  $\mathbf{x}_m \rightarrow \mathbf{x} \in \partial E$ , the limits  $\lim \psi_\gamma(\mathbf{x}_m), \lim D_k \psi_\gamma(\mathbf{x}_m)$  all exist and functions  $\psi_\gamma, D_k \psi_\gamma$  can be extended over all  $E$  in a continuous way. Furthermore, functions  $\{\psi_\gamma\}$  are of class  $C^\infty$  over  $E$ . From now on, we shall consider these functions defined in all  $E$ .
- $0 \leq \psi_\gamma \leq 1, \sum_{\gamma=1}^M \psi_\gamma \equiv 1$  (partition of unity) and  $\psi_\gamma(\mathbf{z}_\zeta) = \delta_{\gamma\zeta}$ .
- Interpolation formula is 1 – *reproductive*. That is, for every linear polynomial  $P$  the following equality holds:

$$P = \sum_{\gamma=1}^M P(\mathbf{z}_\gamma) \psi_\gamma$$

- If  $E$  is an  $n - simplex$ , functions  $\{\psi_\gamma\}$  are the classical linear FEM interpolants.
- Let  $E_{n-1}$  be an  $(n - 1) - facet$  of  $E$  and  $\{\mathbf{z}_{\beta_1}, \dots, \mathbf{z}_{\beta_r}\}$  the subset of *nodes* shared by  $\bar{E}_{n-1}$ . We have

$$\psi_\gamma|_{E_{n-1}} \equiv 0, \text{ if } \gamma \in \{1, \dots, M\} \setminus \{\beta_1, \dots, \beta_r\}$$

Otherwise,  $\psi_\gamma|_{E_{n-1}}$  is obtained from the solution of the  $(n-1)$ -dimensional problem (4) where all data are restricted to the hyperplane generated by  $E_{n-1}$ . In particular, if  $E_{n-1}$  is an  $(n - 1) - simplex$ , functions  $\psi_\gamma|_{E_{n-1}}$  are the standard linear interpolants.

It is this last condition that guarantees continuity of shape functions over a finite element decomposition of a domain  $\bar{\Omega} = \cup E_\alpha$ , where each element  $E_\alpha$  is as in (1).

The partition  $\bar{\Omega} = \cup E_\alpha$  satisfies, of course, the natural condition of FEM:

$$E_\alpha \cap E_\beta = \text{ or }$$

$$E_\alpha \cap E_\beta \text{ is a } (n - 1) - \text{ facet of both } E_\alpha, E_\beta$$

We shall not address here the problem of proving these properties. These calculations are considerably lengthy but the bulk of the work is a careful analysis of the behavior of the rational functions resulting from Gauss procedure in solving (6). These calculations will be presented in a forthcoming paper dealing with error estimates of the interpolants built in this way. Figure 2 shows a shape function over some polyhedral element.

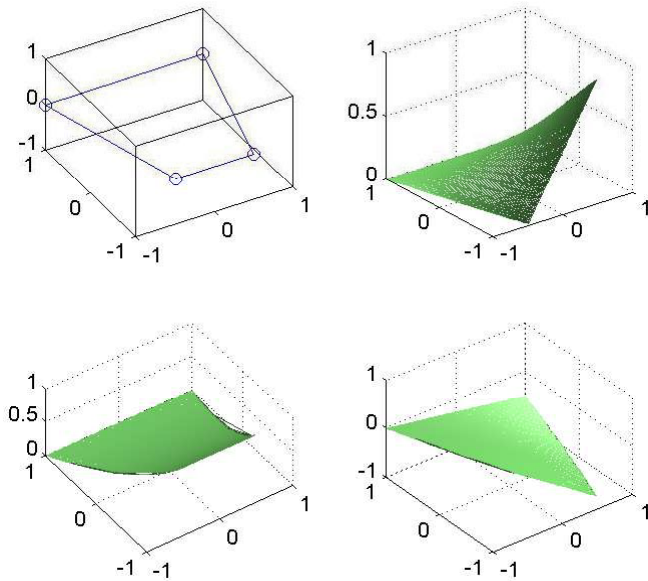


Figure 2: Shape function over a distorted quadrilateral

We should point out that the use of rational functions for finite element interpolation was pioneered by Wachspress<sup>10</sup>, but our use of them is different and gives more accurate results. The rational functions are easily determined by an algorithm based in qhull.

### 3 MORE GENERAL SHAPE FUNCTIONS

The method is not limited to elements with straight *facets* or continuous shape functions.

### 3.1 Curved boundary

Functions  $f_\alpha$  defining the boundary of  $E$  can be any non singular  $C^1$  function. The non-singular function defining the boundary must replace the linear one in (2).

### 3.2 Singular shape functions

In  $E = [(-1, 0), (0, 0), (0, 1), (-1, 1)]$ , we can use, for example, the expression

$$a_0 + a_1 sg(X, Y) + a_2 Y$$

where

$$sg(X, Y) = \sqrt{\sqrt{X^2 + Y^2} - X} \quad (7)$$

in order to get a  $O(\frac{1}{2})$  singularity. Figure 3 shows a shape function build in this way.

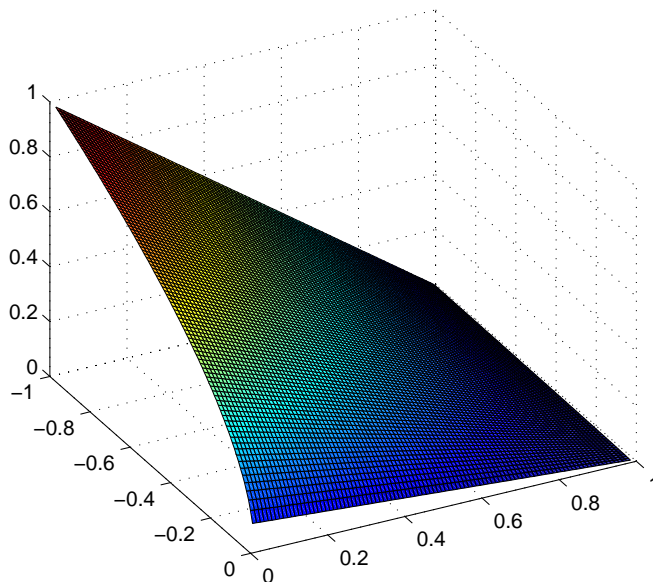


Figure 3: Shape function with a singularity

A gallery of catastrophic shape functions can be constructed in this way<sup>6,7,8</sup>. We must remark, of course, that this kind of shape functions do not have the same properties as in section 2 : they can be discontinuous and lack the reproducing property. We shall pursue this point in a future work.

**Remark 3.2.1** *In all figures, we have calculated shape functions in a strict interior subset of  $E$ . They only suggest the appropriate limit value at the boundary.*

## 4 NUMERICAL EXAMPLES

We shall now perform several numerical tests to investigate the approximating properties of the method in Galerkin scheme. We shall first make all settings in our experiments explicit. Integration on polyhedral is performed using a Delaunay triangulation and a four point integration formula in triangles.

### 4.1 Error measures

The error measure evaluated in all tests is

$$er_{l^2} = \frac{1}{\max_Q |u(\mathbf{x}_\beta)|} \sqrt{\frac{1}{|Q|} |u(\mathbf{x}_\beta) - \hat{u}(\mathbf{x}_\beta)|^2}$$

and, sometimes, the relative absolute maximal error

$$er_\infty = \frac{\max |u(\mathbf{x}_\beta) - \hat{u}(\mathbf{x}_\beta)|}{\max_Q |u(\mathbf{x}_\beta)|}$$

### 4.2 Grids

Several elliptic two dimensional problems have been solved to illustrate the performance of the method. Tests with both random and on uniformly spaced nodes were performed. In the former case, nodes were generated by adding a random perturbation of value  $0.25h$  to a uniform grid with  $h$ -spacing. These kinds of grids will be called *uniform* and *random uniform* grids, respectively. Error displayed in figures in the randomly distributed points case correspond to average over ten runs. In both cases, elements are quadrilateral or deformed quadrilateral.

A more random hybrid grid will be used in model 1. It is generated in the following way:

- First, the boundary of a rectangle is filled with uniformly  $h$ -spaced nodes.
- Interior nodes are aggregated at random with some condition of proximity *aph*. For example, the distance between two nodes can not be lower than  $aph = 0.2h$ . The number of interior nodes is the same as in a uniform grid with  $h$ -spaced nodes.
- A Delaunay triangulation of the nodes is then modified in order to eliminate bad triangles (slivers in dimension three), in such a way that some union of triangles are replaces by polyhedral elements.

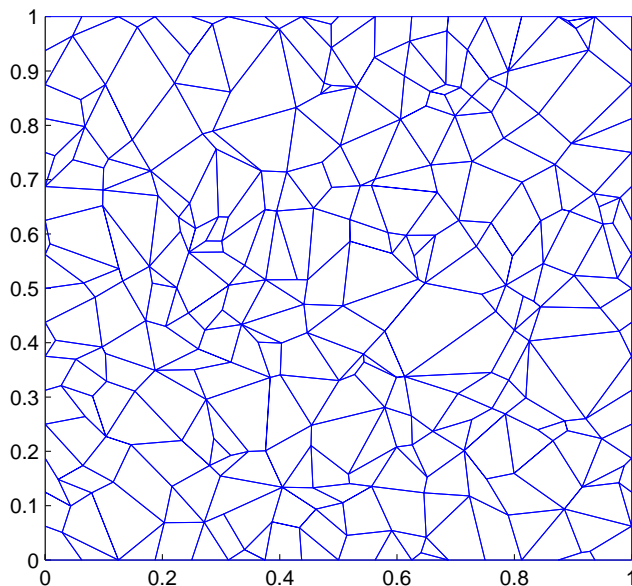


Figure 4: A Random hybrid mesh

Figure 4 depicts a typical *random grid* generated in this way.

We have not worked here in the problem of finding an efficient method for doing this last process, the objective of our tests is to compare the performance of our method with FEM. Certainly, a good algorithm to build this kind of hybrid grid will improve the performance of nemsq. Del Pin<sup>3</sup> deals with this problem in the context of a proposed meshless finite element method where non-Sibsonian interpolants are used in polyhedra.

### 4.3 Dirichlet problem (Poisson equation)

#### 4.3.1 Model 1:

In this case, we put a source that produces a high gradient at the center of the domain. Homogeneous Dirichlet boundary conditions are imposed.

$$\begin{aligned} u_{xx} + u_{yy} &= f(x, y), & \Omega &= \{(x, y) | 0 < x, y < 1\} \\ u|_{\partial\Omega} &= 0 \end{aligned}$$

where

$$f(x, y) = \left( -2ky(1-y) + (ky(1-x)(1-y) - kxy(1-y))^2 - 2kx(1-x) + (kx(1-y)(1-x) - kxy(1-x))^2 \right) \frac{e^{kxy(1-x)(1-y)}}{1 - e^{k/16}}$$

and  $k = 200$  in the tested example. The exact solution to this equation is written

$$u(x, y) = \frac{e^{kxy(1-x)(1-y)}}{1 - e^{k/16}}$$

Figure 5 displays convergence logarithmic plots for nemlsq (our method) and FEM in *uniform* grids.

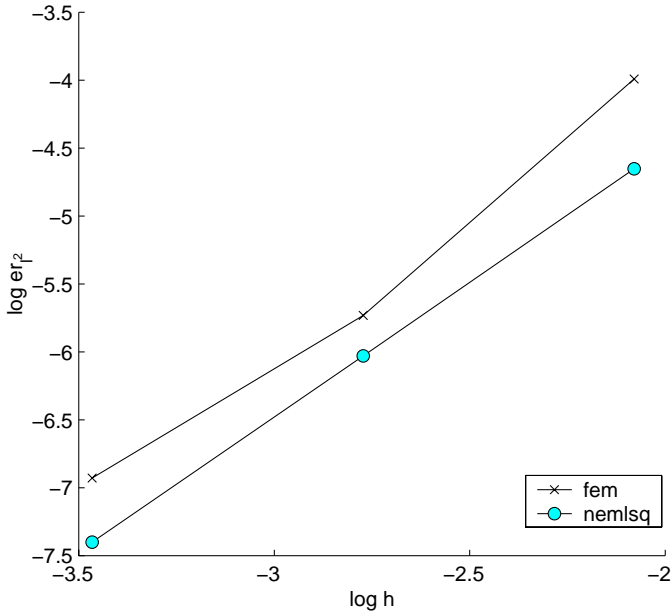


Figure 5: Model 1. Convergence of fem and nemlsq - *uniform* grids

Del Pin et al.<sup>3</sup> used this example to assess the performance of various meshless methods. Figure 6 compares convergence curves for the various methods implemented by Del Pin et al. together with the nemlsq method in *random uniform* grids. In particular, results from linear triangular finite elements (FEM), element free Galerkin (mlsq) with the implementation given of Simonetti<sup>11</sup>, fixed least squares (flsq)<sup>12</sup>, smooth particle hydrodynamics

(shp)<sup>13</sup>, natural element method (nni)<sup>1,2,14</sup>, meshless finite element method (mfem)<sup>3</sup>, and the rational interpolation of Wachspress (wach)<sup>10</sup> in our implementation.

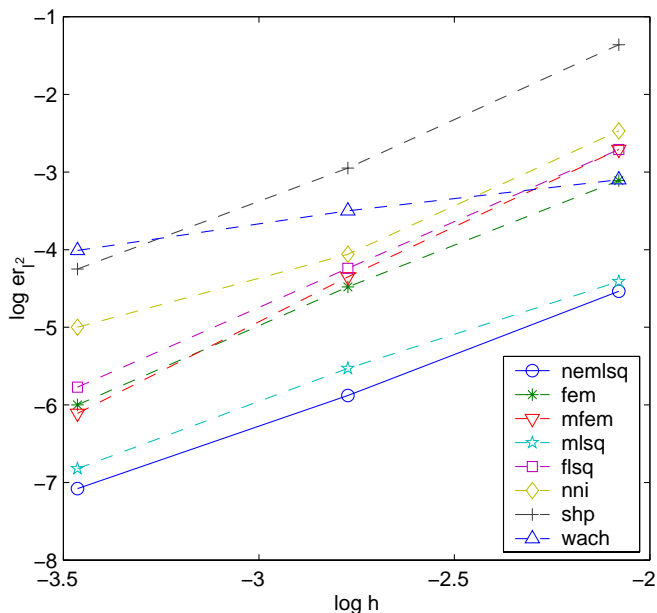


Figure 6: Model 1. *Random uniform grids.*

Figure 7 displays comparative results of nemlsq and FEM in *random grids* with  $aph = 0.2h$ . We can observe the better convergence rate of nemlsq method.

#### 4.4 Singular problems

##### 4.4.1 Model 2:

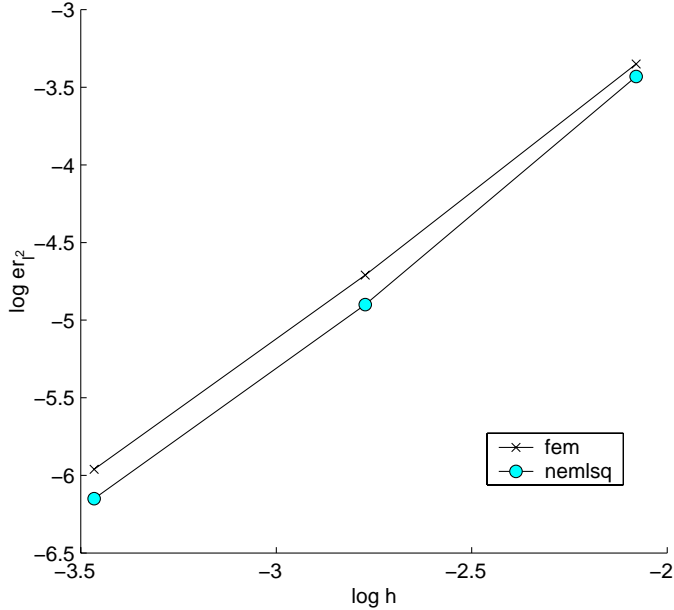
As an example of the use of singular shape functions as in (7), we consider the Dirichlet problem:

$$\begin{aligned} -\Delta u &= 0 & \text{in } \Omega &= (-1, 1) \times (0, 1) \\ u &= s_D & \text{in } \partial\Omega \end{aligned}$$

such that the exact solution is

$$u(x, y) = \sqrt{\sqrt{x^2 + y^2} - x - x^3 - y^3 + 3x^2y + 3xy^2}$$

Figure 8 displays results in *uniform grids* for FEM, nemlsq and nemlsq with the use of

Figure 7: Model 1. Fem and nemlsq - random grids with  $aph = 0.2h$ 

a singular shape function (7) in the left element at  $(0, 0)$  for the error measures  $er_{l^2}$  and  $er_{\infty}$ .

We observe the improvement of results, especially in  $er_{\infty}$ , when the singular shape function is used.

Even the conventional finite element method can be improved with the use of singular shape functions. In fact, our scheme can also be used in triangles. In a FE mesh appropriate for this problem, we obtained the following results:

	$er_{l^2}$	$\max  u - \hat{u} $
conventional FEM :	$2.714e - 4$	$7.43e - 3$
FEM + singular shapes :	$2.221e - 4$	$3.59e - 3$

The singularities are only introduced in the left triangles shared by the node  $(0, 0)$ . We can see that the accuracy has improved.

## 5 CONCLUSIONS

In this investigation we have explored the use of moving least square interpolants and rational weights to generate shape functions in convex polyhedra. The resulting methodology has a number of useful features. Among these, it is an appealing choice to construct

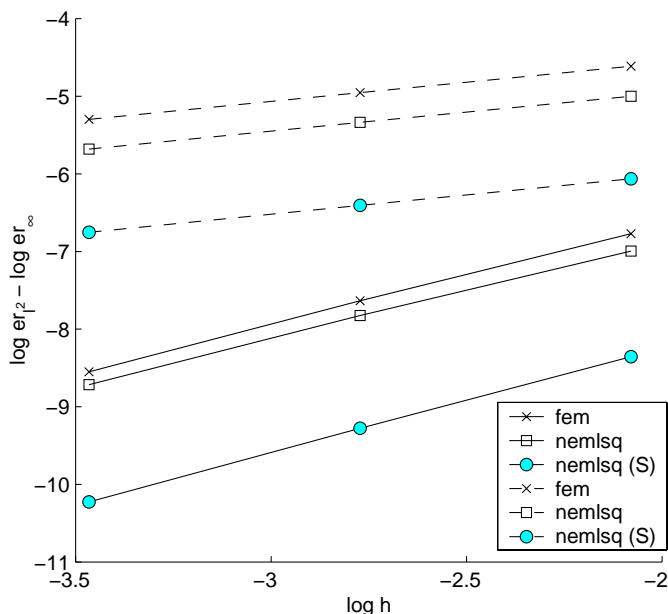


Figure 8: Model 3. Fem and nemlsq - *uniform grids*.  $er_{l2}$  and  $er_{\infty}$  errors

meshless interpolants in the so called meshless finite element method and in general hybrid meshes. The interpolants built in this way appear to produce more accurate results than natural element method, and are less sensitive to mesh distortion.

Applications to problems with singularities are easily handled using singular shape functions and we hope to show in a forthcoming work that this methodology can be used in fracture problems. In all, this hybrid finite element methodology appears to have a number of useful and attractive features that could prove to be important in applications.

## REFERENCES

- [1] Moran B. Sukumar N. and Belytschko T. The natural element method in solid mechanics. *Int. J. Num. Methods Eng.*, **43(5)**, 839–887 (1998).
- [2] Semenov AYu Sukumar N., Moran B. and Belikov VV. Natural neighbor galerkin methods. *Int. J. Num. Methods Eng.*, **50(1)**, 1–27 (2001).
- [3] N. Calvo y M. Storti F. Del Pin F., S. Idelsohn. Comparación del método de elemento finitos con métodos meshless en nubes de puntos random. In Flores F. et al., editor, *Mecánica Computacional - Actas ENIEF*, Córdoba, Argentina, (2001). Asociación Argentina de Mecánica Computacional.

- [4] Petersson A. N. An algorithm for assembling overlapping grid systems. *SIAM J. Sci. Comp.*, **20(6)**, 1995–2022 (1999).
- [5] Dolbow J. Moës N. and Belytschko T. A finite element method for crack growth without remeshing. *Int. J. Num. Methods Eng.*, **46**, 131–150 (1999).
- [6] Zienkiewicz O. C. *The Finite Element Method in Engineering Science*. McGraw-Hill, New York, (1st edn. 1967, 3rd edn. 1977).
- [7] Wait R. and Mitchell R. Corner singularities in elliptic problems by finite element methods. *J. Comp. Phys.*, **8**, 45–52 (1971).
- [8] Mitchell A. *The finite element method in partial differential equations*. John Wiley & Sons, New York, (1977).
- [9] P. Lancaster and K. Salkauskas. *Curve and Surface Fitting. An introduction*. Academic Press, San Diego, (1986).
- [10] Wachspress E. L. *A Rational Finite Element Basis*. Academic Press, New York, (1976).
- [11] G. Simonetti y A. Cardona. Métodos sin malla para resolver la ecuación de conducción del calor. *Revista Internacional de Métodos Numéricos para Cálculo y Diseño en Ingeniería*, **16**, 33–47 (2000).
- [12] O. C. Zienkiewicz R. L. Taylor E. Oñate, S. Idelsohn and C. Sacco. A stabilized finite point method for analysis of fluid mechanics problems. *Comput. Methods Appl. Mech. Engrg.*, **139**, 315–347 (1996).
- [13] S. Koshizuka and Y. Oka. Moving particle semi-implicit method for fragmentation of incompressible fluid. *Nuclear Sc. and Engrg.*, **123**, 421–434 (1996).
- [14] N. Sukumar. *The natural element method in solid mechanics*, (1998).